

FCC-ee Sensitivity to Flavor-Agnostic Standard Model Effective Field Theory Operators

Ben Allanach* and Eetu Loisa†

DAMTP, University of Cambridge, Wilberforce Road, Cambridge, CB3 0WA, United Kingdom

We present a calculation of the sensitivity of the Future Circular e^+e^- Collider (FCC-ee) to the interactions of new, heavy particles in terms of publicly available extensions to the `smelli` and `flavio` computer programs. We parameterize new particles' effects with dimension-6 operators of the Standard Model Effective Field Theory (SMEFT) without any flavor assumptions and take into account the projected experimental and theoretical uncertainties of various electroweak and Higgs observables at the proposed collider. We illustrate a use of the calculation by estimating the sensitivity of the FCC-ee to a family non-universal Z' model that explains anomalies inferred from present-day measurements and Standard Model predictions of observables that involve the $b \rightarrow s\ell^+\ell^-$ transition.

The Future Circular e^+e^- Collider (FCC-ee) is a proposed e^+e^- collider envisaged to be based at CERN [1] and start collisions in the 2040s. It is designed to provide detailed studies of the four most massive particles of the Standard Model (SM): W^\pm bosons, Higgs bosons, Z bosons and top quarks. The FCC-ee affords a significant increase in the precision of measurements of the properties of these heavy particles and sensitivity to rarer decay modes. This enhanced precision enables the exploration of the effects of new particles that may have hitherto evaded detection due to their high mass scale and/or small interaction strengths. Save for certain caveats [2], one may characterize such effects using the Standard Model Effective Field Theory (SMEFT), truncated to a finite order in operator dimension, and obtain a good approximation. The SMEFT Lagrangian density is

$$\mathcal{L} = \mathcal{L}_4 + \sum_{d>4} \sum_i \frac{C_i}{\Lambda^{d-4}} \mathcal{O}_i^{(d)}, \quad (1)$$

where \mathcal{L}_4 is the usual renormalizable SM Lagrangian. The parameter Λ stands for the SMEFT cut-off scale, usually taken to be the mass scale of heavy states that have been integrated out of an underlying renormalizable field theory. The C_i are dimensionless Wilson coefficients (WCs). The index i labels field operators whereas d is the canonical mass dimension of the operator $\mathcal{O}_i^{(d)}$.

The only gauge-invariant dimension-5 operator in the SMEFT expansion, the Weinberg operator [3], describes neutrino masses and mixings. At the dimension-6 level, the number of gauge invariant operators grows into the thousands; these terms describe the physical effects that we are most interested in. A judicious choice of a non-redundant operator basis is important to make sense of the expansion, and we shall henceforth adopt the operators and conventions of the Warsaw basis [4]. Effects of yet higher dimension are suppressed by growing powers of $(E/\Lambda) \ll 1$, where E is the energy scale of the physical process of interest. Since such higher mass dimension operators are generically expected to make smaller impacts on observables, they are not accounted for in

this work. It has been shown (see Fig. 1.12 of Ref. [1]) that, assuming flavor universal new physics couplings, electroweak measurements at the FCC-ee may improve upon the sensitivity of the LHC to certain SMEFT operators by a factor of 4 or so, using present-day theoretical uncertainties. FCC-ee measurements of the Higgs boson may improve the sensitivity on some SMEFT operators by a factor of around 2. In such studies, SMEFT operators, along with their family universal copies, are typically switched on one by one. However, in a specific model which includes heavy fields beyond the SM, many effective operators are typically induced and are highly correlated with each other, being controlled by a small number of fundamental parameters.

We shall present a computational tool that may be used to estimate the sensitivity of the FCC-ee to dimension-6 SMEFT operators in the form of an extension to the `smelli` [5] and `flavio` [6] computer programs. The extension incorporates the projected FCC-ee measurements of Z -pole electroweak observables, fermion scattering above the Z -pole, W boson production and Higgs production, as presented in [7–9]. While the sensitivity of the FCC-ee to WCs with some family universality assumptions has been investigated before [1, 10, 11], to the best of our knowledge, we present the only computational tool with all 2499 dimension-6 general SMEFT WCs included in the estimate of the FCC-ee sensitivity. This makes our work particularly applicable to situations where one is working with new physics models with highly non-trivial flavor structure, such as models explaining flavor anomalies or those resolving the hierarchies in the fermion mass matrices. In such scenarios, it is often necessary to simultaneously fit the model to low energy flavor and high energy electroweak and Higgs data to account for the full set of experimental constraints the model is subject to.

We shall illustrate the use of this tool by providing estimates of the FCC-ee sensitivity to the effects of a TeV-scale Z' boson and flavon, a complex scalar field that spontaneously breaks a $U(1)_{Y_3}$ gauge symmetry, in the Third Family Hypercharge Model (TFHM) [12]. The

TFHM was proposed to explain discrepancies between measurements and SM predictions of processes involving the $b \rightarrow s\ell^+\ell^-$ flavor transition, and so the Z' necessarily is assumed to have flavor-changing and family non-universal interactions. The model can be characterized by the general SMEFT but not by other existing tools that assume various family symmetries of the WCs. The TFHM has further motivation in that the new gauge symmetry provides an explanation for the relative heaviness of the third family of fermions and the smallness of the Cabibbo–Kobayashi–Maskawa mixing angles.

Current bounds on the Z' mass $M_{Z'}$ are $1.2 \text{ TeV} < M_{Z'} < 8.4 \text{ TeV}$ [13]. The lower bound, which comes from direct LHC searches, can be slightly improved upon by the HL-LHC, but it is plausible that no discovery will be forthcoming prior to the FCC-ee. Indirect discovery at the FCC-ee through modifications to the SM prediction of electroweak and Higgs observables would then become a high priority.

PROBING SMEFT USING THE FCC-EE

Recent years have seen a growing interest in estimating the projected experimental sensitivities of various proposed particle accelerators, including the FCC-ee, as well as the constraining power of these measurements on the dimension-6 SMEFT WCs. This section aims to present and discuss the FCC-ee observables incorporated in our newly developed extensions of `flavio v2.6.1` and `smelli v2.4.2`. Where possible, we have followed the principles established in [14].

We adhere to the sensitivity estimates reported in the 2021 Snowmass proceedings [7, 8] and [9]. The assumed running scenario thus corresponds to unpolarized electron and positron beams at center-of-mass energies $\sqrt{s} = 91, 161, 240, 350$ and 365 GeV with luminosities $150, 10, 5, 0.2$ and 1.5 ab^{-1} , respectively. All projected measurements are assumed to be centered on the SM predictions.

The FCC-ee observables are divided into two classes which we shall discuss in the following sections: electroweak precision observables (EWPOs) and Higgs observables. Accessing the newly added observables in `smelli` is straightforward: they are held in some files [15] containing sets of observables and can be included in the instantiation of the global likelihood in `smelli` in the standard way or referenced directly by name through the `flavio` package.

Electroweak precision observables

The FCC-ee would probe the electroweak sector at an unprecedented level of precision, improving upon the current measurements of many observables by two orders of magnitude. Its planned runs at a variety of \sqrt{s} values

ensure experimental sensitivity to a host of SMEFT operators, ranging from four-fermion contact interactions to bosonic field strength operators. Using the estimates of [7] for the FCC-ee measurement uncertainties, we have inserted into the programs FCC-ee uncertainties for the key Z -pole precision observables: the Z boson width, the total hadronic cross-section σ_{had}^0 , the hadronic cross-section ratios R_f and left-right asymmetries A_f . Furthermore, the WW , Zh and $\bar{t}t$ runs allow for precise determinations of many W boson observables, and we include FCC-ee uncertainties for the W boson mass M_W , the W boson width Γ_W , as well as the inclusive WW production cross-sections and leptonic branching ratios $\text{BR}(W \rightarrow \ell\nu)$ measured in the 161, 240 and 365 GeV runs of the collider. The uncertainty estimates for the latter two sets of observables are taken from [9].

The inclusive WW production cross-sections are simulated using the `MadGraph5_aMC` [16] event generator together with the `SMEFTsim` [17, 18] model files. We use the built-in electroweak parton distribution functions [19] on `MadGraph` which account for initial state radiation (and beamstrahlung effects for $\sqrt{s} = 240$ and 365 GeV), turn on WCs one at a time and seek corrections to the SM cross-sections at linear order in the WCs. This amounts to considering the interference terms between the SM amplitude and the SMEFT corrections

$$\sigma = \sigma_{\text{SM}} + \sum_i a_i \frac{C_i}{\Lambda_{\text{UV}}^2} \quad (2)$$

where a_i gives the interference contribution to the cross-section. We include in the cross-sections those SMEFT operators for which

$$\frac{|a_i|}{\sigma_{\text{SM}}} > 10^3 \text{ GeV}^2. \quad (3)$$

Finally, we also include fermion scattering cross-sections and forward-backward asymmetries at $\sqrt{s} = 240$ and 365 GeV for the $e^+e^- \rightarrow \mu^+\mu^-$, $\tau^+\tau^-$, $\bar{c}c$ and $\bar{b}b$ final states, as reported in [7]. These observables excel at probing four-fermion operators because their interference with the SM grows with energy [20, 21]. When applicable, we have cross-checked our analytic calculations with similar results in [22, 23]. The cross-sections are calculated at tree-level and include $\mathcal{O}(\Lambda^{-4})$ corrections in order to account for four-fermion operators that do not interfere with the SM amplitudes. The full set of electroweak observables is collected in Table II.

Higgs measurements

The two leading Higgs production modes at the FCC-ee are $e^+e^- \rightarrow Zh$ (Higgstrahlung) and $e^+e^- \rightarrow h\bar{\nu}\nu$ (W boson fusion), where h stands for the physical Higgs field. The third-most prevalent mode, Z boson fusion,

is tenfold suppressed [8] relative to the first two at the FCC-ee energies 240 GeV and 365 GeV and is neglected. The Higgs measurements are often reported in the form of signal strengths, μ , defined as

$$\mu \equiv \frac{[\sigma_i \cdot \text{BR}(h \rightarrow f)]_{\text{observed}}}{[\sigma_i \cdot \text{BR}(h \rightarrow f)]_{\text{SM}}}, \quad (4)$$

for a given h production mode cross-section σ_i and branching ratio $\text{BR}(h \rightarrow f)$ into final state f .

Again, `MadGraph` and `SMEFTsim` are employed to simulate the dominant Higgs production modes at the FCC-ee, following precisely the same procedure as outlined above for WW production. These are then normalized to their SM predictions to derive signal strengths. The full set of Higgs observables can be found in Table III.

Treatment of theory errors

In order to translate the vast improvements in experimental precision at the FCC-ee into tests of the SM, it is imperative that the theory errors nor the relevant observables are improved to match the experimental precision. Both parametric theory errors, arising from the finite measurement precision of the SM input parameters, and intrinsic theory errors, emerging from missing higher order contributions in the SM theory predictions for various observables, must be controlled. The feasibility of sufficiently large improvements in time for the FCC-ee were the subject of [24, 25], where it was deemed that with a concerted effort, the theory errors may be brought down to match the experimental precision for the observables considered in this letter. Furthermore, explicit estimates for the parametric and theory uncertainties were given by the authors. We have incorporated these estimates into the FCC-ee observables introduced here. When projected theoretical uncertainties for a given observable are unavailable, we assume the total theoretical uncertainty matches the projected experimental error, unless the current theoretical error is smaller, in which case we adopt the present-day value.

We add the parametric and intrinsic theory uncertainties to the projected experimental uncertainties for the EWPOs and Higgs observables in quadrature. This implicitly assumes that the three sources of uncertainty are uncorrelated, which should hold to a reasonable degree. Our procedure also implicitly treats the theory uncertainty as a Gaussian random variable. This makes our procedure operationally simple, as other treatments would likely require dedicated changes to the core `flavio` program.

All projected experimental uncertainties are treated as uncorrelated. As for the theory errors, whenever the predicted values of two observables are obviously correlated, we treat them as such. Thus, for instance, we take into account that the cross-sections $\sigma(e^+e^- \rightarrow \mu^+\mu^-)$

and $\sigma(e^+e^- \rightarrow \tau^+\tau^-)$ rely on the same theory prediction, as do the Higgs signal strength predictions for a given production mode but different decay channels. Where the correlation between two theory predictions is approximately one, we treat the theory errors as fully correlated. For example, we therefore treat the theory errors in $\sigma(e^+e^- \rightarrow \mu^+\mu^-)$ at $\sqrt{s} = 240$ GeV and at $\sqrt{s} = 365$ GeV as fully correlated.

The estimation and implementation of both projected experimental and theory errors is not an exact science. We caution that our estimates are subject to refinement over the coming decades prior to FCC-ee operation.

AN ILLUSTRATION: FITS OF THE THIRD FAMILY HYPERCHARGE MODEL

We now demonstrate our new code with a use-case: that of estimating the sensitivity of the FCC-ee to a particular new physics model that explains discrepancies between certain measurements and SM predictions of B meson decay observables. The Third Family Hypercharge Model (TFHM) [12] extends the SM gauge group by a $U(1)_{Y_3}$ factor under which the third family fermions and the Higgs boson have charges proportional to their hypercharge, but under which the other SM fields are uncharged. $U(1)_{Y_3}$ is spontaneously broken around the TeV scale by a SM singlet complex scalar field, the flavon, θ , which takes on a vacuum expectation value (VEV) v_θ . As a result, the Z' gauge boson which mediates the new interaction acquires a mass, $M_{Z'}$. Despite being coupled to only the *third* generation of SM fermions in the gauge eigenbasis, the Z' acquires interactions with the lighter fermion species when the fermions are rotated into the mass eigenbasis; an angle θ_{sb} , for example, parameterizes the mixing between the left-handed strange and bottom quark fields. This allows the novel gauge boson to mediate $b \rightarrow s\ell^+\ell^-$ transitions via Feynman diagrams that, after matching to the SMEFT, yield four-fermion operators suppressed by the ratio $C_i/\Lambda^2 \sim g_{Z'}^2/M_{Z'}^2$, with $g_{Z'}$ being the $U(1)_{Y_3}$ gauge coupling. Furthermore, as the Higgs field H is charged under both $U(1)_Y$ and $U(1)_{Y_3}$, the Z boson and the Z' mix with mixing angle α_z ,

$$\sin \alpha_z = \frac{g_{Z'}}{\sqrt{g_L^2 + g_Y^2}} \left(\frac{M_Z}{M_{Z'}} \right)^2 + \mathcal{O} \left(\frac{M_Z^4}{M_{Z'}^4} \right), \quad (5)$$

at tree-level.

To leading order, two parameters of the TFHM determine its ability to fit B meson decay data: the ratio $g_{Z'}/M_{Z'}$ and θ_{sb} . Whilst the $b \rightarrow s\ell^+\ell^-$ anomaly landscape has evolved over the recent years (see the review [26]), the ability of the TFHM to improve the fit to the anomalous B meson decay measurements endures. In order to show this, we construct a global likelihood consisting of three sets of observables. The ‘Quarks’ data set

contains various rare B meson decay observables, some of which are in tension with the SM, as well as neutral meson mixing and other commonly studied flavor observables. The data set ‘LFU FCNCs’ consists of measurements testing lepton flavor universality, including the formerly anomalous R_K and R_{K^*} , and ‘EWPOs’ is made up of Z - and W -pole electroweak observables. The best-fit point of the resulting fit improves upon the SM by 29.1 units of χ^2 [27]. The results are summarised in Table I, which updates the fit presented in [28].

TABLE I. The goodness of fit of the TFHM at its best-fit point, $\{g_{Z'} = 0.412, \theta_{sb} = -0.182\}$, when $M_{Z'}$ is set to 3 TeV. From left to right, the columns show the names of the observable sets used, the ensuing χ^2 values, the number of observables in each set and finally the improvement in χ^2 relative to the SM fit, with positive values signalling an improved fit.

Data set	χ^2	n	p -value	$\Delta\chi^2$
Quarks	393.8	306	5.14×10^{-4}	29.45
LFU FCNCs	19.0	24	0.75	-0.43
EWPOs	36.9	31	0.22	0.08
Global	449.4	361	1.0×10^{-3}	29.10

Another point of interest is the scalar sector of the Lagrangian. Aside from the mass terms and quartic self-interaction terms that generically exist for both the Higgs field H and the flavon field θ , the symmetries of the model allow for a marginal interaction term between the scalars, $\lambda_{H\theta}(H^\dagger H)(\theta^*\theta)$. As a result, integrating out the heavy flavon from the theory yields a contribution to the dimension-six bosonic operator $(H^\dagger H)\square(H^\dagger H)$, which in the broken electroweak phase and under canonical normalization of the physical, real Higgs field results in the rescaling of all Higgs couplings in the SM (see for instance [29]). This operator can also be viewed as capturing the mixing between the physical Higgs and flavon in the scalar mass matrix, necessitating a rotation into a new scalar mass basis. The mixing angle required to diagonalise the mass matrix reads, in terms of the Lagrangian parameters,

$$\sin 2\phi = \frac{2\lambda_{H\theta}v_H v_\theta}{m_\theta^2 - m_h^2}, \quad (6)$$

where v_θ and v_H are the VEVs of the flavon and Higgs fields, respectively, with m_θ and m_h being their respective physical masses.

The Z' leaves an imprint on the EWPOs (a detailed discussion of the fit to present-day EWPO data can be found in [28]), not least because the custodial symmetry of the SM is now violated. Furthermore, the Higgs-flavon mixing, governed by the angle ϕ , influences the electroweak sector through one-loop effects, in addition to its tree-level impact on Higgs production processes. These features make the model susceptible to constraints

from both electroweak and Higgs production observables, measurable at current colliders as well as the FCC-ee.

Figure 1 shows the expected improvement in precision of constraints on the model from Higgs observables and EWPOs at the FCC-ee in a plane of TFHM parameter space. The SM point lies at the origin: we see initially that the ‘Quarks + LFU’ region, preferred by B meson decay data, is far from this point, but that current Higgs and EWPO measurements are compatible with it. The figure also illustrates the improvement in precision and sensitivity once FCC-ee measurements are taken into account. Supposing the SM to be the theory chosen by Nature, the TFHM region of parameter space currently preferred the ‘Quarks + LFU’ data (which includes the anomalous B decays) would be strongly disfavored by the FCC-ee.

Both current and projected electroweak measurements show a mild degeneracy, where increasing $g_{Z'}$ and ϕ simultaneously allows for a mixing angle larger than when the gauge coupling is zero. This is because an increased Higgs-flavon mixing angle acts to lower M_W , whilst increased $g_{Z'}$ makes the W boson heavier. It is these opposite sign contributions to M_W , whose experimental world average (prior to the 2022 CDF measurement) is in 2σ tension with the SM [30], that give rise to this behaviour.

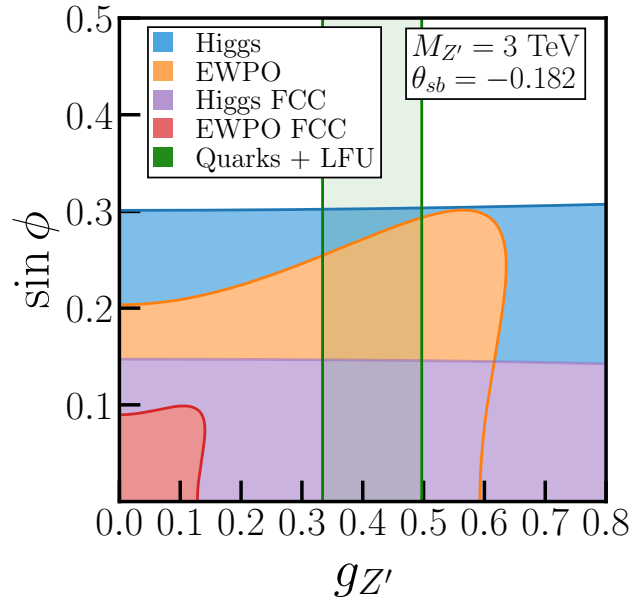


FIG. 1. 95% confidence level (CL) contours of the TFHM in the $\sin\phi - g_{Z'}$ plane for $M_{Z'} = 3$ TeV and $\theta_{sb} = -0.182$. The plot shows current constraints and SM-centered FCC-ee projections. The colored region corresponding to the legend is ‘allowed’ for each class of observables: that of ‘Quarks + LFU’ shows the current 95% region preferred by the fit to B meson data; ‘Higgs’ and ‘EWPO’ refer to current constraints. Legend items including the word ‘FCC’ show FCC-ee sensitivity estimates.

CLOSING REMARKS

We have extended the `smelli` and `flavio` computer packages to provide an estimate of the FCC-ee sensitivity to general (i.e. including family dependent) dimension-6 SMEFT operators. Some pioneering work on ‘low-hanging fruit’ of correlated theoretical uncertainties has been performed as part of the extensions. To illustrate the use of the new features, we have shown how the TFHM can be highly constrained indirectly by electroweak and Higgs measurements at the FCC-ee. The FCC-ee is expected to deliver 10^{12} B mesons [31], allowing for a further increase in precision on the measurement of processes involving the $b \rightarrow s\mu^+\mu^-$ transition. This may lead to the abandonment or further tweaking of the TFHM, since such processes were a large part of the initial motivation for it; in either case, indirect measurements at the FCC-ee will lead our direction beyond (or indeed back to) the SM.

We hope to improve the code in many ways in the future. Several more observables could be added, for instance those derived from $t\bar{t}$ production at the FCC-ee. Inserting differential Higgs and W production observables into the programs would help break degenerate directions in the SMEFT parameter space, thus refining these tools. Furthermore, it would be useful to study the correlations between various intrinsic theory errors in greater detail and to insert estimates of the correlations among the experimental uncertainties.

The features introduced here could be straightforwardly extended to other proposed e^+e^- colliders, and we hope to do so in the future. In addition to e^+e^- colliders comparable to the FCC-ee, a similar analysis could

be conducted for the proposed TeV scale muon colliders, although the domain of validity of the SMEFT approach would be smaller because a muon collider would operate at a larger \sqrt{s} , which new physics degrees of freedom must be more massive than. We believe that high-energy physics stands to benefit greatly from the development of accessible and automated tools for comparing the sensitivities of various proposed colliders to a range of concrete extensions of the SM. In this letter, we hope to have taken a meaningful step towards that goal.

ACKNOWLEDGMENTS

We thank other members of the Cambridge Pheno Working Group for discussions. EL would like to thank Peter Stangl, Alex Mitov and Daniel Yeo for helpful suggestions. This work has been partially supported by STFC consolidated grants ST/X000664/1 and ST/T000694/1.

List of FCC-ee observables

Tables II and III of this appendix display the full sets of Higgs and electroweak observables introduced in this letter. Whenever an observable is defined at many different center-of-mass energies, \sqrt{s} is treated as an extra parameter for the EWPOs, whereas \sqrt{s} appears in the name of the Higgs signal strength observables. This feature, which results from striving to modify the existing `flavio` program as minimally as possible, explains the differences in the naming conventions between the two tables.

* ben.allanach.work@gmail.com

† eal47@cam.ac.uk

- [1] A. Abada *et al.* (FCC), *Eur. Phys. J. ST* **228**, 261 (2019).
- [2] Such caveats are that the energy scale of the observables in question are far below the mass scale of any new particles and that the linearly-realised SM Higgs doublet field is the only one which contributes to electroweak symmetry breaking.
- [3] S. Weinberg, *Phys. Rev. Lett.* **43**, 1566 (1979).
- [4] B. Grzadkowski, M. Iskrzynski, M. Misiak, and J. Rosiek, *JHEP* **10**, 085 (2010), arXiv:1008.4884 [hep-ph].
- [5] J. Aebischer, J. Kumar, P. Stangl, and D. M. Straub, *Eur. Phys. J. C* **79**, 509 (2019), arXiv:1810.07698 [hep-ph].
- [6] D. M. Straub, (2018), arXiv:1810.08132 [hep-ph].
- [7] J. de Blas, Y. Du, C. Grojean, J. Gu, V. Miralles, M. E. Peskin, J. Tian, M. Vos, and E. Vryonidou, in *Snowmass 2021* (2022) arXiv:2206.08326 [hep-ph].

-
- [8] G. Bernardi *et al.*, (2022), arXiv:2203.06520 [hep-ex].
 - [9] J. De Blas, G. Durieux, C. Grojean, J. Gu, and A. Paul, *JHEP* **12**, 117 (2019), arXiv:1907.04311 [hep-ph].
 - [10] T. Giani, G. Magni, and J. Rojo, *Eur. Phys. J. C* **83**, 393 (2023), arXiv:2302.06660 [hep-ph].
 - [11] E. Celada, T. Giani, J. ter Hoeve, L. Mantani, J. Rojo, A. N. Rossia, M. O. A. Thomas, and E. Vryonidou, *JHEP* **09**, 091 (2024), arXiv:2404.12809 [hep-ph].
 - [12] B. C. Allanach and J. Davighi, *JHEP* **12**, 075 (2018), arXiv:1809.01158 [hep-ph].
 - [13] B. C. Allanach, J. M. Butterworth, and T. Corbett, *JHEP* **08**, 106 (2019), arXiv:1904.10954 [hep-ph].
 - [14] A. Falkowski and D. Straub, *JHEP* **04**, 066 (2020), arXiv:1911.07866 [hep-ph].
 - [15] The extensions are held in the Github repositories https://github.com/eetuloisa/smelli_fcc and https://github.com/eetuloisa/flavio_fcc. The FCC-ee features can currently be accessed by making local copies of the two repositories. When using `smelli`, the new observables are contained in the files `likelihood_ewpt_fccee.yaml` and `likelihood_higgs_fccee.yaml`.

TABLE II. The electroweak precision observables in `flavio` and `smelli` whose projected measurements have been added to the programs. The first column shows the name of the observable, the second its name in the code and the third a brief description.

	Observable	Name in program	Description
Z-pole observables	Γ_Z	GammaZ	Total Z boson decay width
	σ_{had}^0	sigma_had	Cross-section $\sigma(e^+e^- \rightarrow \text{hadrons})$ at the Z -pole
	A_e	A(Z->ee)	Left-right asymmetry in $Z \rightarrow e^+e^-$ decays
	A_μ	A(Z->mumu)	Left-right asymmetry in $Z \rightarrow \mu^+\mu^-$ decays
	A_τ	A(Z->tautau)	Left-right asymmetry in $Z \rightarrow \tau^+\tau^-$ decays
	A_b	A(Z->bb)	Left-right asymmetry in $Z \rightarrow \bar{b}b$ decays
	A_c	A(Z->cc)	Left-right asymmetry in $Z \rightarrow \bar{c}c$ decays
	R_e	R_e	Partial decay width $\Gamma_{Z \rightarrow ee}$ relative to hadronic width
	R_μ	R_mu	Partial decay width $\Gamma_{Z \rightarrow \mu\mu}$ relative to hadronic width
	R_τ	R_tau	Partial decay width $\Gamma_{Z \rightarrow \tau\tau}$ relative to hadronic width
	R_b	R_b	Partial decay width $\Gamma_{Z \rightarrow bb}$ relative to hadronic width
	R_c	R_c	Partial decay width $\Gamma_{Z \rightarrow cc}$ relative to hadronic width
	Super-Z-pole fermion scattering	$\sigma(e^+e^- \rightarrow e^+e^-)$	sigma(ee->ee) (high_E)
$A_{\text{FB}}(e^+e^- \rightarrow e^+e^-)$		AFB(ee->ee) (high_E)	Forward-backward asymmetry in $e^+e^- \rightarrow e^+e^-$; $\sqrt{s} = 240, 365$ GeV
$\sigma(e^+e^- \rightarrow \mu^+\mu^-)$		sigma(ee->mumu) (high_E)	Cross-section of $e^+e^- \rightarrow \mu^+\mu^-$; $\sqrt{s} = 240, 365$ GeV
$A_{\text{FB}}(e^+e^- \rightarrow \mu^+\mu^-)$		AFB(ee->mumu) (high_E)	Forward-backward asymmetry in $e^+e^- \rightarrow \mu^+\mu^-$; $\sqrt{s} = 240, 365$ GeV
$\sigma(e^+e^- \rightarrow \tau^+\tau^-)$		sigma(ee->tautau) (high_E)	Cross-section of $e^+e^- \rightarrow \tau^+\tau^-$; $\sqrt{s} = 240, 365$ GeV
$A_{\text{FB}}(e^+e^- \rightarrow \tau^+\tau^-)$		AFB(ee->tautau) (high_E)	Forward-backward asymmetry in $e^+e^- \rightarrow \tau^+\tau^-$; $\sqrt{s} = 240, 365$ GeV
$\sigma(e^+e^- \rightarrow \bar{b}b)$		sigma(ee->bb) (high_E)	Cross-section of $e^+e^- \rightarrow \bar{b}b$; $\sqrt{s} = 240, 365$ GeV
$A_{\text{FB}}(e^+e^- \rightarrow \bar{b}b)$		AFB(ee->bb) (high_E)	Forward-backward asymmetry in $e^+e^- \rightarrow \bar{b}b$; $\sqrt{s} = 240, 365$ GeV
Super-Z-pole fermion scattering	$\sigma(e^+e^- \rightarrow \bar{c}c)$	sigma(ee->cc) (high_E)	Cross-section of $e^+e^- \rightarrow \bar{c}c$; $\sqrt{s} = 240, 365$ GeV
	$A_{\text{FB}}(e^+e^- \rightarrow \bar{c}c)$	AFB(ee->cc) (high_E)	Forward-backward asymmetry in $e^+e^- \rightarrow \bar{c}c$; $\sqrt{s} = 240, 365$ GeV
W boson observables	M_W	m_W	Pole mass of the W boson
	Γ_W	GammaW	Width of the W boson
	$R(e^+e^- \rightarrow W^+W^-)$	R(ee->WW)	Inclusive WW production cross-section normalized to SM prediction; $\sqrt{s} = 161, 240, 365$ GeV
	$\text{BR}(W \rightarrow e\nu)$	BR(W->enu)	W boson branching ratio into $e\nu$
	$\text{BR}(W \rightarrow \mu\nu)$	BR(W->munu)	W boson branching ratio into $\mu\nu$
	$\text{BR}(W \rightarrow \tau\nu)$	BR(W->taunu)	W boson branching ratio into $\tau\nu$

- [16] J. Alwall, R. Frederix, S. Frixione, V. Hirschi, F. Maltoni, O. Mattelaer, H. S. Shao, T. Stelzer, P. Torrielli, and M. Zaro, *JHEP* **07**, 079 (2014), arXiv:1405.0301 [hep-ph].
- [17] I. Brivio, Y. Jiang, and M. Trott, *JHEP* **12**, 070 (2017), arXiv:1709.06492 [hep-ph].
- [18] I. Brivio, *JHEP* **04**, 073 (2021), arXiv:2012.11343 [hep-ph].
- [19] S. Frixione, O. Mattelaer, M. Zaro, and X. Zhao, (2021), arXiv:2108.10261 [hep-ph].
- [20] L. Berthier and M. Trott, *JHEP* **05**, 024 (2015), arXiv:1502.02570 [hep-ph].
- [21] S.-F. Ge, Z. Qian, M. J. Ramsey-Musolf, and J. Zhou, (2024), arXiv:2410.17605 [hep-ph].
- [22] A. Greljo, J. Salko, A. Smolkovič, and P. Stangl, *JHEP* **05**, 087 (2023), arXiv:2212.10497 [hep-ph].
- [23] B. Allanach and A. Mullin, *JHEP* **09**, 173 (2023), arXiv:2306.08669 [hep-ph].
- [24] A. Freitas *et al.*, (2019), arXiv:1906.05379 [hep-ph].
- [25] A. Blondel, A. Freitas, J. Gluza, T. Riemann, S. Heinemeyer, S. Jadach, and P. Janot, (2019), arXiv:1901.02648 [hep-ph].
- [26] B. Capdevila, A. Crivellin, and J. Matias, *Eur. Phys. J. ST* **1**, 20 (2023), arXiv:2309.01311 [hep-ph].
- [27] For $M_{Z'}$ = 3 TeV, we find a best-fit point of $\theta_{sb} = -0.182$ and $g_{Z'} = 0.412$ for a normalization in which the $U(1)_{Y_3}$ charge of the third-family left-handed quark doublet is 1/6. The fit accounts for the renormalization group running of the EFT operators by numerically integrating the dimension-6 renormalization group equations. This is made possible by the `wilson` program [32].
- [28] B. C. Allanach, J. E. Camargo-Molina, and J. Davighi,

TABLE III. The Higgs signal strength observables whose projected measurements were added into the programs. The first column shows the name of the observable, whereas the second column gives its name in the code. The notation $\{240|365\}$ means that the observable is defined for two values of \sqrt{s} , one of which should be specified by the user.

Observable	Name in program
$\mu(e^+e^- \rightarrow Zh; h \rightarrow \bar{b}b)$	mu_Zh_{240 365}(h->bb)
$\mu(e^+e^- \rightarrow Zh; h \rightarrow \bar{c}c)$	mu_Zh_{240 365}(h->cc)
$\mu(e^+e^- \rightarrow Zh; h \rightarrow gg)$	mu_Zh_{240 365}(h->gg)
$\mu(e^+e^- \rightarrow Zh; h \rightarrow ZZ)$	mu_Zh_{240 365}(h->ZZ)
$\mu(e^+e^- \rightarrow Zh; h \rightarrow WW)$	mu_Zh_{240 365}(h->WW)
$\mu(e^+e^- \rightarrow Zh; h \rightarrow \tau\tau)$	mu_Zh_{240 365}(h->tautau)
$\mu(e^+e^- \rightarrow Zh; h \rightarrow \gamma\gamma)$	mu_Zh_{240 365}(h->gammagamma)
$\mu(e^+e^- \rightarrow Zh; h \rightarrow Z\gamma)$	mu_Zh_240(h->Zgamma)
$\mu(e^+e^- \rightarrow Zh; h \rightarrow \mu\mu)$	mu_Zh_{240 365}(h->mumu)
$\mu(e^+e^- \rightarrow h\nu\nu; h \rightarrow \bar{b}b)$	mu_hnunu_{240 365}(h->bb)
$\mu(e^+e^- \rightarrow h\nu\nu; h \rightarrow \bar{c}c)$	mu_hnunu_365(h->cc)
$\mu(e^+e^- \rightarrow h\nu\nu; h \rightarrow gg)$	mu_hnunu_365(h->gg)
$\mu(e^+e^- \rightarrow h\nu\nu; h \rightarrow ZZ)$	mu_hnunu_365(h->ZZ)
$\mu(e^+e^- \rightarrow h\nu\nu; h \rightarrow WW)$	mu_hnunu_365(h->WW)
$\mu(e^+e^- \rightarrow h\nu\nu; h \rightarrow \tau\tau)$	mu_hnunu_365(h->tautau)
$\mu(e^+e^- \rightarrow h\nu\nu; h \rightarrow \gamma\gamma)$	mu_hnunu_365(h->gammagamma)
$\mu(e^+e^- \rightarrow h\nu\nu; h \rightarrow \mu\mu)$	mu_hnunu_365(h->mumu)

Eur. Phys. J. C **81**, 721 (2021), arXiv:2103.12056 [hep-ph].

[29] R. Alonso, E. E. Jenkins, A. V. Manohar, and M. Trott, JHEP **04**, 159 (2014), arXiv:1312.2014 [hep-ph].

[30] S. Navas *et al.* (Particle Data Group), Phys. Rev. D **110**, 030001 (2024).

[31] A. Abada *et al.* (FCC), Eur. Phys. J. C **79**, 474 (2019).

[32] J. Aebischer, J. Kumar, and D. M. Straub, Eur. Phys. J. C **78**, 1026 (2018), arXiv:1804.05033 [hep-ph].